BMC Cardiovascular Disorders

RESEARCH

Open Access

U-shaped association between plasma cyclic guanosine monophosphate-adenosine monophosphate (cGAMP) levels and myocardial infarction

Quan Zhang[1], Huiqing Ding[1], Zhongling Dai[1], Rukai Yang[1], Shenghua Zhou[1] and Shi Tai[1*]

Abstract

Background The cyclic guanosine monophosphate-adenosine monophosphate synthase-stimulator of interferon genes (cGAS-STING) signaling pathway is closely associated with myocardial infarction (MI). Cyclic guanosine monophosphate-adenosine monophosphate (cGAMP) is a key component of this pathway; however, there is currently a lack of clinical evidence linking plasma cGAMP levels to MI.

Methods This study utilized clinical data from 270 patients diagnosed with coronary heart disease (CHD) at the Second Xiangya Hospital of Central South University. The outcomes included ST-segment elevation and non-ST-segment elevation MI. Univariate and multivariate logistic regression models were used to explore the relationships between plasma cGAMP levels and MI, while restricted cubic spline (RCS) using logistic regression to explore the dose-response relationship.

Results Among the 270 patients, the mean plasma cGAMP level was 1352.58 ± 106.02 ng/L and 89 (32.96%) patients were diagnosed with MI. The RCS curves indicated a U-shape association between the cGAMP levels and MI; the risk of MI was negatively correlated with the cGAMP until it hit bottoms at 1352 ng/L. When the cGAMP level exceeded 1352 ng/L, the risk of MI increased significantly (adjusted OR, 1.02; 95% CI: 1.01–1.03). When considering cGAMP as a categorical variable, patients in Tertile 1 and Tertile 3 had a 167% (adjusted OR: 2.67, 95% CI: 1.23–5.78) and 155% (adjusted OR: 2.55, 95% CI: 1.17–5.55) higher risk of MI compared to those in Tertile 2, respectively. These results were consistent across subgroup analyses, notably, a significant interaction by age category was observed in patients with cGAMP ≥ 1352 ng/L, where the positive association was pronounced in the elderly.

Conclusions A U-shaped association exists between cGAMP and MI in the CHD population, with a cutoff point at the cGAMP of 1352 ng/L. Both excessively high and low cGAMP levels are associated with an increased risk of MI, particularly among the elderly with cGAMP ≥ 1352 ng/L. This is the first clinical evidence of the cGAS-cGAMP-STING pathway in metabolic cardiovascular diseases.

ClinicalTrials.gov Identifier NCT03363035 (Registration date: 2018-01-15).

*Correspondence:
Shi Tai
taishi2017@csu.edu.cn

Full list of author information is available at the end of the article

Keywords cGAS-STING, cGAMP, Metabolic cardiovascular disease, Myocardial infarction

Introduction

Metabolic cardiovascular diseases are characterized by significant cardiovascular dysfunction, underpinned by pathological processes such as impaired glucose and lipid metabolism, heightened immune-inflammatory responses, oxidative stress, and endothelial dysfunction, these processes collectively contribute to long-term mortality in affected populations [1, 2]. Atherosclerotic cardiovascular disease is the primary pathophysiological basis of metabolic cardiovascular diseases, of which myocardial infarction (MI) is the most severe form, thus identifying potential intervention targets binding metabolism and cardiovascular diseases may be important for promote global health.

The cyclic GMP-AMP synthase-stimulator of interferon genes (cGAS-STING) signaling pathway is intricately linked to a variety of metabolic cardiovascular diseases, including atherosclerosis (AS) [3–5], myocardial hypertrophy and fibrosis [6–8], aortic aneurysm and dissection [9–11]. Previous research reveals that DNA damage is frequently observed in endothelial cells, smooth muscle cells, and macrophages within atherosclerotic plaques [12], which can be detected by cGAS, resulting in the activation of inflammatory cytokines and alterations in cellular phenotypes. However, cGAS-STING pathway is also associated with autophagy, which is essential for clearing necrotic cells and tissue debris, this may help myocardial repair during myocardial infarction (MI) [13]. Thus, elucidating the complex relationship between cGAS-STING pathway and MI will contribute to develop new therapeutic strategy for preventing metabolic cardiovascular diseases.

Cyclic guanosine monophosphate-adenosine monophosphate (cGAMP), as the second messenger of cGAS-STING pathway, was synthesized by cGAS from adenosine triphosphate (ATP) and guanosine triphosphate (GTP), and bound to and activated the protein STING [14–16], this may be a promising monitoring markers for cGAS-STING pathway. However, clinical evidence linking plasma cGAMP levels to metabolic cardiovascular diseases remains limited. To address this gap, we conducted a retrospective study aimed at exploring the potential association between plasma cGAMP levels and MI in patients with coronary heart disease (CHD).

Materials and methods

Patient population

The study utilized clinical data from 340 patients diagnosed with CHD at the chest pain center of the Second Xiangya Hospital of Central South University, collected between January and July 2022. The clinical data included laboratory test results, prescriptions, diagnoses, physical examination findings, and laboratory test. This project was approved by the ethics committee of the Second Xiangya Hospital of Central South University and all patients provided written informed consent.

The exclusion criteria were as follows: (a) Estimated glomerular filtration rate (eGFR) less than 60 mL/min/1.73m^2 ($n = 44$). (b) Severe hepatic insufficiency ($n = 8$). (c) A life expectancy of less than one year ($n = 10$). (d) Severe infection ($n = 8$). Finally, a total of 270 patients were included in the final analysis (Fig. 1).

Study outcomes

The primary outcome of this study was acute myocardial infarction, including ST-segment elevation MI (STEMI) and non-ST-segment elevation MI (NSTEMI). All diagnoses of myocardial infarction were confirmed by experienced cardiologists based on symptoms, laboratory tests, and coronary angiography.

Quantification of cGAMP

The concentration of cGAMP was quantified using an enzyme-linked immunosorbent assay (ELISA) (FANKEW, Cat. No. F11293-A). Microplates were coated with purified human cGAMP antibodies to establish a solid-phase antibody layer. cGAMP standards and samples were then added, allowing binding to monoclonal antibodies. HRP-conjugated cGAMP antibodies were introduced to form an antibody-antigen-enzyme complex. After thorough washing to eliminate unbound components, the substrate TMB was added for color development. HRP catalyzed the conversion of TMB to a blue product, which turned yellow upon the addition of an acid stop solution. The color intensity, directly proportional to the cGAMP concentration, was measured at 450 nm using a microplate reader, and concentrations were determined based on a standard curve.

Statistical analysis

All analyses were conducted using R (v4.2.2, www.R-project.org) and IBM SPSS Statistics (v22.0, IBM Corp., Armonk, NY, USA). A P-value < 0.05 was considered statistically significant.

There were missing values in serum creatinine (SCr, $n = 5$), Hemoglobin (Hb, $n = 5$), cardiac troponin T (cTNT, $n = 2$), N-Terminal Pro-Brain Natriuretic Peptide (NT-pro BNP, $n = 10$), Hb1Ac ($n = 3$), the "missForest" R software package was utilized for imputing missing value. For sensitive analysis, we conduct additional mean imputation (Supplement Tables 1, 2 and 3, Supplement Fig. 1).

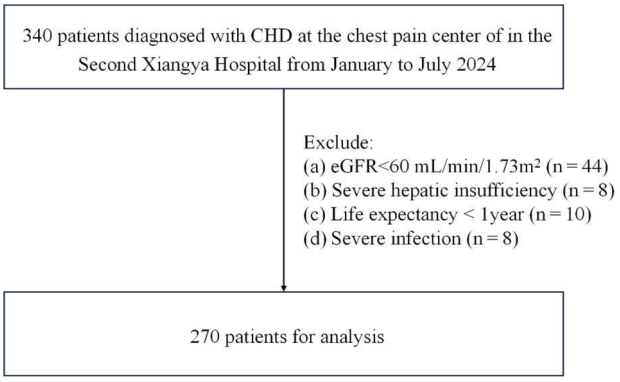

Fig. 1 Flowchart of study population selection. The study utilized clinical data from 340 patients diagnosed with CHD at the chest pain center of the Second Xiangya Hospital of Central South University, collected between January and July 2024. The exclusion criteria were as follows: (**a**) Estimated glomerular filtration rate (eGFR) less than 60 mL/min/1.73m^2 ($n=44$). (**b**) Severe hepatic insufficiency ($n=8$). (**c**) A life expectancy of less than one year ($n=10$). (**d**) Severe infection ($n=8$). Finally, a total of 270 patients were included in the final analysis

Baseline characteristics are reported as frequencies with corresponding percentages for categorical variables. Continuous variables are presented as mean ± standard deviation for normally distributed data, while for non-normally distributed data, a median with an interquartile range was used. Normality was assessed using normal Q-Q plots. One-way ANOVA (for normally distributed values), Kruskal-Wallis H-test (for data with skewed distribution), and chi-square test (for categorical variables) are used to compare the clinical characteristics in different tertiles.

Univariate and multivariate logistic regression models were used to explore the relationships between cGAMP and MI, and odd ratios (ORs) were expressed with their 95% confidence intervals (95% CIs). We conducted the models to biased yielded caused by multi-collinearity estimates. The model 1 adjusted for age, sex, hypertension, diabetes, smoking, drinking. The model 2 further adjusted for all statistically significantly variables in Table 1 and the univariate logistic regression model for MI in the CHD population including body mass index (BMI), systolic blood pressure (SBP), left ventricular ejection fraction (LVEF), Creatinine, cardiac troponin (cTNT), N-terminal pro-brain natriuretic peptides (NT-pro BNP), High-Density Lipoprotein (HDL), apolipoprotein A1 (apo-A1), FFA (free fatty acids). We further conducted subgroup tests in all possible subgroups and for 6 clinically important interaction terms in the univariate logistic regression models for sensitive analysis (sex, age, BMI, hypertension, diabetes, smoking).

The "rms" R software package was used to generate restricted cubic splines. We used restricted cubic spline (RCS) logistic regression (adjusted for variables in Model 2), to explore the dose–response relationship between the cGAMP and MI, the optimal model was selected based on the Bayesian Information Criterion.

Results

Baseline characteristics between different groups

Baseline characteristics of the study population stratified by cGAMP levels are presented in Table 1 and Supplement Table 1. Of the 270 patients, 212 (78.52%) were male, with a median age of 61.83 ± 10.78 years and a mean plasma cGAMP level of 1352.58 ± 106.02 ng/L. Compared to patients in tertile 2, more patients in tertiles 1 and 3 were diagnosed with myocardial infarction, no significant difference of other variables were observed. Similar results were found when we allocated patients to two groups according to 1352 ng/L (Supplement Table 4).

Univariate logistic regression model for myocardial infarction

In total, 89 patients (32.96%) were diagnosed with myocardial infarction. The results of the univariate logistic regression model for MI, presented in Table 2, show that elevated levels of HDL, apoA1, and LVEF were negatively correlated with the occurrence of MI, suggesting a protective effect. On the other hand, higher levels of free fatty acids, cTNT, NT-pro BNP, creatinine, as well as a history of hypertension, were significantly positively associated with the increased risk of MI in the CHD population.

cGAMP and the risk of myocardial infarction

After multivariable adjustment, RCS curves revealed a U-shaped association between cGAMP and MI, with a threshold of 1352 ng/L (P for non-linearity < 0.001, Fig. 2). This indicates distinct associations between cGAMP and MI above and below the cutoff point. Specifically, in patients with cGAMP levels ≥ 1352 ng/L, each unit increase in cGAMP was associated with a 2% higher risk of MI (adjusted OR 1.02, 95% CI 1.01–1.03, $P=0.003$). Conversely, although not statistically significant, in patients with cGAMP levels < 1352 ng/L, each unit increase in cGAMP was associated with a 1% lower risk of MI (adjusted OR 0.99, 95% CI 0.99-1.00, $P=0.113$) (Table 3). When considering cGAMP as a categorical variable, patients in Tertile 1 had a 167% higher risk of MI compared to those in Tertile 2 (adjusted OR: 2.67, 95% CI: 1.23–5.78, $P=0.013$). Similarly, patients in Tertile 3 had a 155% higher risk of MI (adjusted OR: 2.55, 95% CI: 1.17–5.55, $P=0.013$) (Table 3). The ROC curve analysis demonstrated that cGAMP exhibits robust predictive power for MI (Fig. 3).

Sensitivity analyses across six subgroups showed similar results (Figs. 4 and 5). Notably, a significant interaction by age category was observed in patients with cGAMP ≥ 1352 ng/L, where the positive association

Table 1 Baseline characteristics of patients in different tertiles

Variables	Total ($n=270$)	Tertile 1 ($n=90$)	Tertile 2 ($n=90$)	Tertile 3 ($n=90$)	*P*
cGAMP, ng/L	1352.58 ± 106.02	1227.54 ± 37.44	1359.28 ± 38.58	1470.93 ± 32.57	< 0.001
CHD category					0.037
Stable angina	77 (28.52)	23 (25.56)	26 (28.89)	28 (31.11)	
Unstable angina	104 (38.52)	31 (34.44)	45 (50.00)	28 (31.11)	
NSTEMI	38 (14.07)	18 (20.00)	5 (5.56)	15 (16.67)	
STEMI	51 (18.89)	18 (20.00)	14 (15.56)	19 (21.11)	
Demographics					
Age, years	61.62 ± 10.49	61.27 ± 11.87	60.96 ± 10.18	62.63 ± 9.31	0.523
Male, %	212 (78.52)	19 (21.11)	19 (21.11)	20 (22.22)	0.978
BMI, kg/m^2	24.88 ± 3.45	25.22 ± 3.32	24.54 ± 3.76	24.88 ± 3.27	0.418
SBP, mmHg	129.18 ± 18.90	127.02 ± 15.95	129.76 ± 19.38	130.76 ± 21.04	0.392
DBP, mmHg	80.14 ± 12.97	79.39 ± 12.23	81.01 ± 14.25	80.03 ± 12.43	0.701
HR, beats/min	76.08 ± 13.16	76.17 ± 13.44	75.30 ± 13.98	76.78 ± 12.08	0.752
Current smoker, %	153 (56.67)	49 (54.44)	59 (65.56)	45 (50.00)	0.095
Drinking history, %	56 (20.74)	18 (20.00)	16 (17.78)	22 (24.44)	0.532
NYHA class III-IV, %	80 (29.63)	24 (26.67)	27 (30.00)	29 (32.22)	0.714
LVEF, %	57.56 ± 9.56	56.29 ± 10.57	59.02 ± 8.40	57.36 ± 9.48	0.154
Comorbidity					
Hypertension, %	177 (65.56)	59 (65.56)	56 (62.22)	62 (68.89)	0.642
Diabetes, %	112 (41.48)	38 (42.22)	41 (45.56)	46 (51.11)	0.482
Stroke, %	36 (13.33)	6 (6.67)	15 (16.67)	15 (16.67)	0.075
Atrial fibrillation, %	39 (14.44)	15 (16.67)	9 (10.00)	15 (16.67)	0.340
Laboratory test					
Hemoglobin, g/L	137.65 ± 14.73	138.81 ± 14.30	137.62 ± 13.91	136.52 ± 15.97	0.582
Creatinine, mmol/L	82.34 ± 20.28	83.48 ± 23.08	82.04 ± 19.19	81.50 ± 18.45	0.797
eGFR, ml/min/1.73m^2	92.35 ± 26.85	91.56 ± 22.72	92.17 ± 27.36	93.31 ± 30.20	0.907
ALB, g/L	40.05 ± 4.38	39.70 ± 5.58	40.11 ± 3.44	40.33 ± 3.86	0.621
Potassium, mmol/L	4.02 ± 0.35	4.02 ± 0.38	4.01 ± 0.34	4.02 ± 0.33	0.984
CK, U/L	128.43 ± 195.62	133.25 ± 241.63	132.92 ± 195.11	119.13 ± 138.14	0.859
CK-Mb, U/L	21.27 ± 18.43	23.95 ± 27.41	19.90 ± 12.50	19.95 ± 10.28	0.239
cTNT, ng/L	127.36 ± 376.37	149.71 ± 371.41	97.83 ± 307.60	134.54 ± 440.61	0.638
NT-pro BNP, pg/ml	679.52 ± 1493.62	765.13 ± 1260.28	524.18 ± 1395.45	749.25 ± 1780.59	0.482
Glucose, mmol/L	5.58 ± 1.54	5.57 ± 1.41	5.55 ± 1.60	5.62 ± 1.61	0.957
Hb1Ac, %	6.91 ± 1.28	6.92 ± 1.18	6.94 ± 1.43	6.87 ± 1.22	0.919
Triglyceride, mmol/L	1.90 ± 1.44	2.07 ± 2.02	1.77 ± 0.93	1.87 ± 1.15	0.360
TCHO, mmol/L	3.72 ± 1.15	3.84 ± 1.44	3.63 ± 1.07	3.68 ± 0.88	0.430
LDL, mmol/L	2.09 ± 0.93	2.10 ± 1.02	2.06 ± 0.98	2.11 ± 0.79	0.932
HDL, mmol/L	1.02 ± 0.23	1.05 ± 0.25	1.01 ± 0.25	1.00 ± 0.21	0.319
LP (a), mg/L	246.77 ± 283.83	237.73 ± 295.07	290.38 ± 307.87	212.19 ± 241.73	0.170
APO-A1, g/L	1.11 ± 0.18	1.13 ± 0.19	1.10 ± 0.20	1.11 ± 0.16	0.593
APO-B, g/L	0.66 ± 0.23	0.67 ± 0.25	0.65 ± 0.24	0.66 ± 0.19	0.815
FFA, umol/L	0.39 ± 0.17	0.39 ± 0.14	0.39 ± 0.14	0.40 ± 0.22	0.981
Medications					
ACEI, %	4 (1.48)	1 (1.11)	0 (0.00)	3 (3.33)	0.328
ARB, %	39 (14.44)	13 (14.44)	15 (16.67)	11 (12.22)	0.698
SGLT2i, %	88 (32.59)	28 (31.11)	31 (34.44)	29 (32.22)	0.889
Metformin, %	30 (11.11)	8 (8.89)	14 (15.56)	8 (8.89)	0.259
Beta blockers, %	167 (61.85)	56 (62.22)	54 (60.00)	57 (63.33)	0.896
CCB, %	52 (19.26)	15 (16.67)	13 (14.44)	24 (26.67)	0.086
Statins, %	246 (91.11)	81 (90.00)	80 (88.89)	85 (94.44)	0.383

ACEI: angiotensin-converting enzyme inhibitor; ALB: albumin; APO-A1: apolipoprotein A1; APO-B: apolipoprotein B; ARB: angiotensin II receptor blocker; BMI: body mass index; CCB: calcium channel blocker; CK: creatine kinase; CK-Mb: creatine kinase-MB (myocardial band); cTNT: cardiac troponin T; DBP: diastolic blood pressure; eGFR: estimated glomerular filtration rate; FFA: free fatty acids; HbA1c: hemoglobin A1c (glycated hemoglobin); HDL: high-density lipoprotein; HR: heart rate; LDL: low-density lipoprotein; LP (a): lipoprotein (a); LVEF: left ventricular ejection fraction; NSTEMI: non-ST-segment elevation MI; NT-pro BNP: N-terminal pro-brain natriuretic peptide; NYHA: New York Heart Association functional class; SBP: systolic blood pressure; SGLT2i: sodium-glucose cotransporter 2 inhibitor; STEMI: ST-segment elevation MI; TCHO: total cholesterol

Table 2 Univariate logistic regression model for myocardial infarction

Variables	OR (95CI%)	*P*
Demographics		
Age	0.99 (0.96 ~ 1.01)	0.267
Female	0.89 (0.48 ~ 1.67)	0.724
BMI	1.09 (1.01 ~ 1.18)	0.021
SBP	0.99 (0.98 ~ 1.01)	0.308
DBP	0.99 (0.97 ~ 1.01)	0.530
HR	0.99 (0.98 ~ 1.01)	0.559
Current smoker	1.19 (0.71 ~ 2.00)	0.503
Drinking history	1.56 (0.85 ~ 2.87)	0.149
NYHA class, III-IV	1.14 (0.66 ~ 1.98)	0.644
LVEF	0.96 (0.93 ~ 0.98)	0.002
Comorbidity		
Hypertension	2.79 (1.54 ~ 5.06)	< 0.001
Diabetes	1.48 (0.89 ~ 2.46)	0.133
Stroke	1.02 (0.48 ~ 2.15)	0.960
Atrial fibrillation	1.33 (0.66 ~ 2.68)	0.431
Laboratory test		
Hemoglobin	1.00 (0.98 ~ 1.02)	0.780
Creatinine	1.02 (1.01 ~ 1.03)	0.006
eGFR	1.00 (0.99 ~ 1.01)	0.924
ALB	1.04 (0.98 ~ 1.11)	0.213
Potassium	1.16 (0.56 ~ 2.39)	0.692
CK	1.00 (1.00 ~ 1.00)	0.108
CK-Mb	1.01 (0.99 ~ 1.03)	0.187
cTNT	1.01 (1.01 ~ 1.01)	0.002
NT-pro BNP	1.01 (1.01 ~ 1.01)	< 0.001
Glucose	1.04 (0.89 ~ 1.23)	0.598
Hb1Ac	1.06 (0.87 ~ 1.29)	0.553
Triglyceride	1.06 (0.89 ~ 1.25)	0.531
TCHO	1.13 (0.91 ~ 1.41)	0.255
LDL	1.16 (0.89 ~ 1.53)	0.273
HDL	0.22 (0.06 ~ 0.74)	0.014
LP (a)	1.00 (1.00 ~ 1.00)	0.124
APO-A1	0.21 (0.05 ~ 0.94)	0.041
APO-B	2.84 (0.92 ~ 8.79)	0.070
FFA	5.77 (1.22 ~ 27.40)	0.027
Medications		
ACEI	0.67 (0.07 ~ 6.58)	0.734
ARB	0.77 (0.36 ~ 1.63)	0.495
Beta blockers	1.07 (0.63 ~ 1.81)	0.800
CCB	1.10 (0.58 ~ 2.07)	0.778
Statins	0.80 (0.34 ~ 1.91)	0.621
Metformin	1.02 (0.46 ~ 2.28)	0.963
SGLT2i	1.00 (0.58 ~ 1.72)	0.998

ACEI: angiotensin-converting enzyme inhibitor; ALB: albumin; APO-A1: apolipoprotein A1; APO-B: apolipoprotein B; ARB: angiotensin II receptor blocker; BMI: body mass index; CCB: calcium channel blocker; CK: creatine kinase; CK-Mb: creatine kinase-MB (myocardial band); cTNT: cardiac troponin T; DBP: diastolic blood pressure; eGFR: estimated glomerular filtration rate; FFA: free fatty acids; HbA1c: hemoglobin A1c (glycated hemoglobin); HDL: high-density lipoprotein; HR: heart rate; LDL: low-density lipoprotein; LP (a): lipoprotein (a); LVEF: left ventricular ejection fraction; NT-pro BNP: N-terminal pro-brain natriuretic peptide; NYHA: New York Heart Association functional class; SBP: systolic blood pressure; SGLT2i: sodium-glucose cotransporter 2 inhibitor; TCHO: total cholesterol

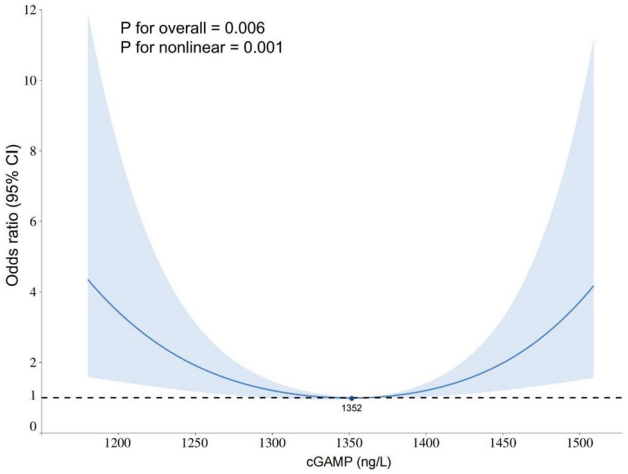

Fig. 2 Relationship between the cGAMP and the risk of MI based on restricted cubic spline curves. There is a U-shaped association exists between cGAMP and MI in the CHD population. ORs are based on a multivariate logistic regression model. CI = confidence interval, MI = myocardial infarction, OR = odds ratio

between cGAMP and MI was particularly pronounced in elderly individuals.

Discussion

Two key conclusions can be drawn from our study. Firstly, a U-shaped association exists between cGAMP levels and myocardial infarction in the CHD population, with a threshold of 1352 ng/L. Secondly, elevated cGAMP level was associated with an increased risk of MI in patients with cGAMP ≥ 1352 ng/L after multivariate adjustment, particularly among elderly.

To our knowledge, this is the first clinical evidence for the research of the cGAS-cGAMP-STING pathway in metabolic cardiovascular diseases. Our research confirms the critical role of the cGAS-cGAMP-STING pathway in metabolic cardiovascular diseases and highlights the predictive value of cGAMP in CHD populations.

The interaction between age category and the relationship between cGAMP and MI is intriguing. One of our latest results indicated that STING activation accelerating macrophage senescence and vascular aging [17]. Previous researches also shown that various aging triggers, including oxidative stress, radiation, oncogene activation, and pharmacological induction, can activate the cGAS-STING pathway and induce senescence-associated secretory phenotype expression [18–21]. All of these suggests that the activation of the cGAS-STING pathway may be a common feature of cellular aging, this kind of higher baseline elevated cGAMP level makes the relationship between cGAMP and MI more evident in elderly patients.

The positive association between cGAMP and MI aligns with our expectations. The mechanisms underlying

Table 3 Risk of MI in CHD patients in different cGAMP groups

cGAMP (ng/L)	Crude model HR (95% CI)	*P* values	Model 1 HR (95% CI)	*P* values	Model 2 HR (95% CI)	*P* values
As continuous variable						
< 1352	0.99 (0.99-1.00)	0.022	0.99 (0.98-1.00)	0.038	0.99 (0.98-1.00)	0.113
≥ 1352	1.01 (1.00-1.02)	0.013	1.02 (1.00-1.02)	0.003	1.02 (1.01–1.03)	0.003
As categorical variable						
Tertile 1 (< 1293)	2.49 (1.29–4.82)	0.007	2.75 (1.37–5.50)	0.004	2.67 (1.23–5.78)	0.013
Tertile 2 (1293–1422)	Ref	/	Ref	/	Ref	/
Tertile 3 (> 1422)	2.27 (1.17–4.40)	0.015	2.33 (1.16–4.70)	0.018	2.55 (1.17–5.55)	0.018

Model 1 adjusted for age, sex, hypertension, diabetes, smoking, drinking

Model 2 adjusted for age, sex, hypertension, diabetes, smoking, drinking, BMI, SBP, LVEF, Creatinine, cTNT, NT-pro BNP, HDL, apo-A1, FFA

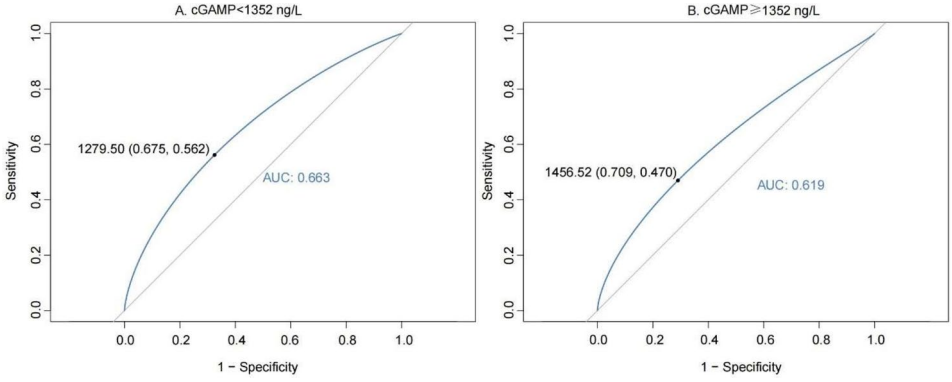

Fig. 3 Receiver operating characteristic curves for myocardial infarction. The ROC curve analysis demonstrated that cGAMP exhibits robust predictive power for MI

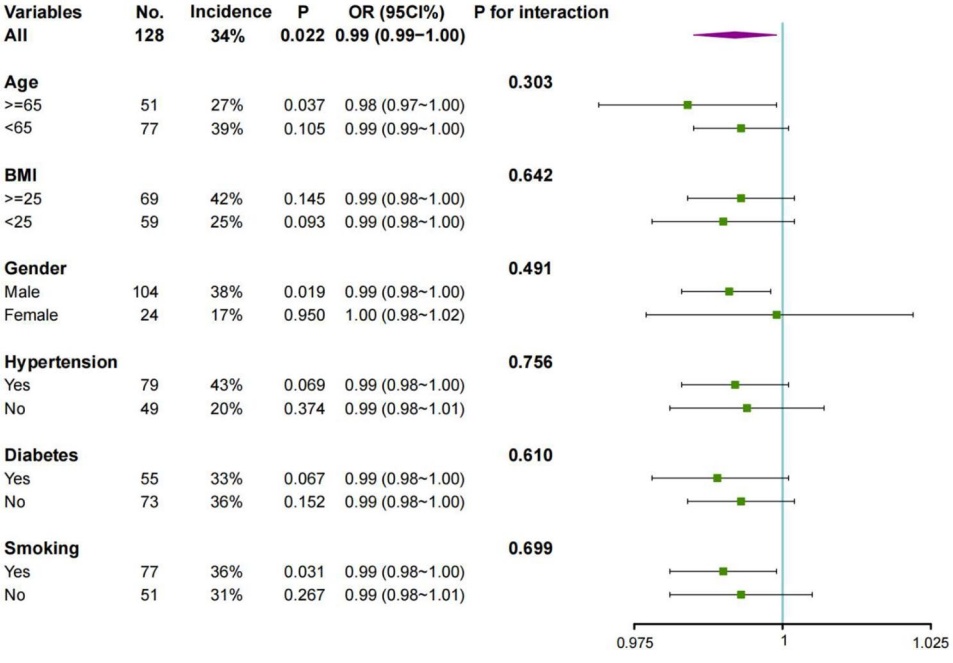

Fig. 4 Subgroup analyses for myocardial infarction in patients with cGAMP < 1352 ng/L. Elevated cGAMP was associated with lower risk of MI in patients with cGAMP < 1352 ng/L and no significant interaction were found in all subgroups. CI = confidence interval, MI = myocardial infarction, OR = odds ratio

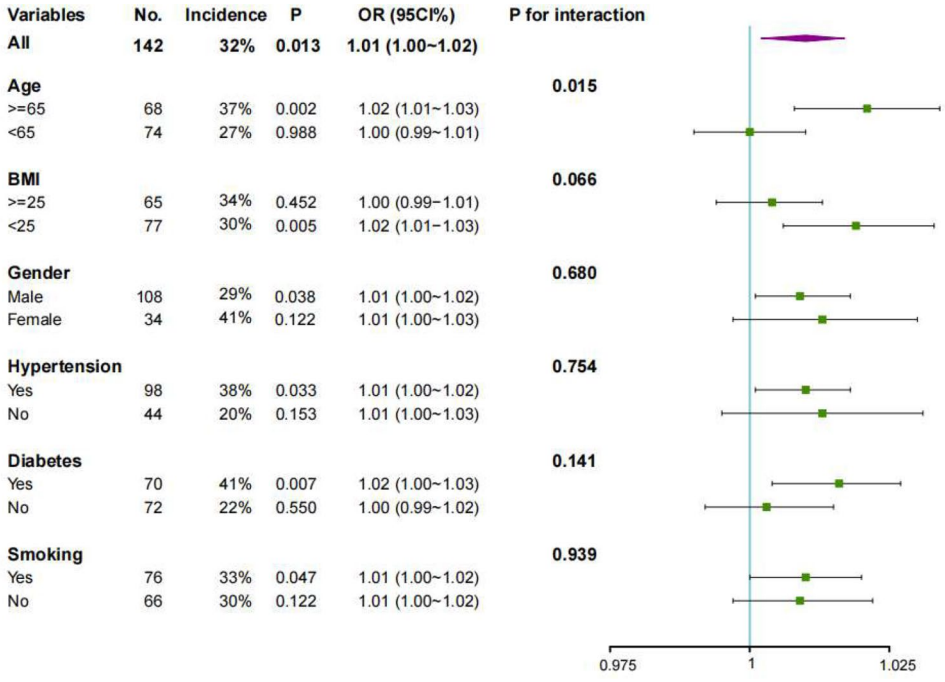

Fig. 5 Subgroup analyses for myocardial infarction in patients with cGAMP ≥ 1352 ng/L. Elevated cGAMP was associated with higher risk of MI in patients with cGAMP ≥ 1352 ng/L and significant interaction by age category was observed, the positive association between cGAMP and MI was particularly pronounced in elderly individuals. CI = confidence interval, MI = myocardial infarction, OR = odds ratio

this association can be attributed to several factors across different cell types: Firstly, hyperactivation of the cGAS-STING pathway can lead to programmed cell death of cardiomyocyte. Studies have shown that zidovudine triggers mitochondrial stress, causing mitochondrial DNA leakage into the cytoplasm, which activates the cGAS-STING pathway and leads to excessive autophagy, intracellular lipid peroxidation, and ultimately autophagy-dependent ferroptosis [22]. Lysosomal cell death induced by the cGAS-STING pathway is also an important mechanism of programmed cell death [23]. Secondly, hyperactivation of the cGAS-STING pathway in macrophages promotes the expression of various inflammatory cytokines through the TBK1-IRF3 and NF-κB pathways, as well as synergistic inflammatory signaling via TLRs and STAT. This kind of prolonged inflammation drives macrophage to pro-inflammatory M1 phenotype polarization, contributing to lipid deposition, adverse remodeling, and the progression of atherosclerosis [24, 25]. Thirdly, activation of the cGAS-STING-IFN pathway promotes the phenotypic switching of vascular smooth muscle cells (VSMCs) through autocrine and paracrine mechanisms [26]. Moreover, activation of the cGAS-STING pathway induces the phosphorylation and inactivation of the transcription factor YAP1 and impairs cyclin D gene transcription, leading to the suppression of endothelial cell proliferation [27]. This not only directly damages endothelial cells, resulting in a reduction of fibrous cap-forming VSMCs and thinning of the fibrous cap, leading to the destabilization of atherosclerotic plaques [26], but also impairs the endothelial cells' ability to regulate vascular tone, ultimately accelerating the progression of atherosclerosis [3, 28]. Last but not least, disruption of blood flow followed MI further exacerbates inflammatory responses and immune cell infiltration, macrophage-mediated phagocytosis of necrotic cells and cellular debris promotes MI progression through STING-IRF3 activation. Substantial differences were observed in ventricular remodeling and survival between WT mice and $IRF3^{-/-}$, $IFNAR^{-/-}$ or $cGAS^{-/-}$ mice [29, 30]. Platelet cGAS depletion also ameliorated myocardial ischemia-reperfusion injury [31].

Given that the complicated relationship between autophagy and MI [13], the association between cGAMP and MI in patients with cGAMP < 1352 ng/L was unexpected yet within reasons. On one hand, autophagy exacerbates ischemia/reperfusion injury [32], on the other hand, evidence suggesting that autophagy plays an important role in cardiomyocyte repair during MI [33, 34]; Therefore, as a classic autophagy-activating pathway, maintaining a certain level of activation of the cGAS-STING pathway aids in the removal of abnormal DNA, damaged organelles, thereby promoting cellular renewal and maintaining cellular and tissue homeostasis in MI [35, 36], while pathway attenuation may impair this primitive yet essential function. Thus, targeting the cGAS-STING pathway may represent a promising therapeutic strategy for treating MI.

The strength of this study lies in its inclusion of a diverse cohort of CHD patients, which enhances the generalizability of the findings. Subgroup analyses further reinforced the robustness of our results. However, several limitations should be acknowledged. First, as a retrospective study, causal relationships between cGAMP and MI cannot be established. Second, this is a single-center study conducted in China, limiting the generalizability of the findings to other populations. Lastly, the absence of long-term follow-up data precludes further investigation into the relationship between cGAMP and long-term prognosis in CHD patients, thus our findings require validation in larger, multicenter studies.

Conclusions

This study is an early exploration of the clinical relevance of cGAMP, there is a U-shaped association exists between cGAMP and MI in the CHD population, elevated cGAMP was associated with an increased risk of MI in patients with cGAMP ≥ 1352 ng/L. The results provide robust clinical evidence for the research of the cGAS-cGAMP-STING pathway in metabolic cardiovascular diseases.

Abbreviations

ACEI	Angiotensin-Converting Enzyme Inhibitor
ALB	Albumin
APO-A1	Apolipoprotein A1
APO-B	Apolipoprotein B
ARB	Angiotensin II Receptor Blocker
AS	Atherosclerosis
BMI	Body Mass Index
CCB	Calcium Channel Blocker
cGAMP	Cyclic guanosine monophosphate-adenosine monophosphate
cGAS	Cyclic guanosine monophosphate-adenosine monophosphate
CHD	Coronary Heart Disease
CK	Creatine Kinase
CK-Mb	Creatine Kinase-MB
cTNT	cardiac Troponin T
DBP	Diastolic Blood Pressure
eGFR	estimated Glomerular Filtration Rate
FFA	Free Fatty Acids
HbA1c	Hemoglobin A1c
HDL	High-Density Lipoprotein
HR	Heart Rate
MI	Myocardial Infarction
LDL	Low-Density Lipoprotein
LP (a)	Lipoprotein (a)
LVEF	Left Ventricular Ejection Fraction
NSTEMI	non-ST-segment elevation MI
NT-pro BNP	N-terminal pro-brain natriuretic peptide
NYHA	New York Heart Association functional class
SBP	Systolic Blood Pressure
STEMI	ST-segment Elevation MI
SGLT2i	Sodium-Glucose cotransporter 2 inhibitor
STING	Synthase-Stimulator of Interferon Gene
TCHO	Total Cholesterol

Supplementary Information

The online version contains supplementary material available at https://doi.org/10.1186/s12872-025-04543-9.

Supplementary Material 1

Acknowledgements

We thank the editors and the reviewers for their useful feedback that improved this paper.

Author contributions

This study was completed in collaboration with the following authors: SZ and ST defined the study themes and methods; QZ and HD analyzed the data; QZ and ZD wrote the paper; and RY and ST edited the manuscript. All authors have read and approved the final manuscript.

Funding

This work was supported by the National Natural Science Foundation of China (82271601, 81801394 to Shi Tai).

Data availability

All data included in this study are available upon request by contact with the corresponding author.

Declarations

Ethics approval and consent to participate

This study followed the Helsinki Declaration principles and ethical approval was granted by the Hunan Provincial Hospital ethics committee. The authors confirm that patient consent forms have been obtained for this article.

Consent for publication

All authors listed above approved the manuscript for publication.

Competing interests

The authors declare no competing interests.

Author details

[1]Department of Cardiovascular Medicine, The Second Xiangya Hospital, Central South University, Changsha, Hunan 410011, China

Received: 30 September 2024 / Accepted: 31 January 2025
Published online: 19 February 2025

References

1. Kim MK, Han K, Park Y-M, Kwon H-S, Kang G, Yoon K-H, Lee S-H. Associations of variability in blood pressure, glucose and cholesterol concentrations, and body Mass Index with Mortality and Cardiovascular outcomes in the General Population. Circulation. 2018;138:2627–37. https://doi.org/10.1161/CIRCULATIONAHA.118.034978.
2. Mouton AJ, Li X, Hall ME, Hall JE. Obesity, hypertension, and Cardiac Dysfunction: Novel roles of Immunometabolism in Macrophage activation and inflammation. Circ Res. 2020;126:789–806. https://doi.org/10.1161/CIRCRESAHA.119.312321.
3. Liu Q, Cheng Z, Huang B, Luo S, Guo Y. Palmitic acid promotes endothelial-to-mesenchymal transition via activation of the cytosolic DNA-sensing cGAS-STING pathway. Arch Biochem Biophys. 2022;727:109321. https://doi.org/10.1016/j.abb.2022.109321.
4. Uryga AK, Grootaert MOJ, Garrido AM, Oc S, Foote K, Chappell J, Finigan A, Rossiello F, d'Adda di Fagagna F, Aravani D., Jorgensen H.F., Bennett M.R. Telomere damage promotes vascular smooth muscle cell senescence and immune cell recruitment after vessel injury. Commun Biol. 2021;4:611. https://doi.org/10.1038/s42003-021-02123-z.
5. Kwak H, Lee E, Karki R. DNA sensors in metabolic and cardiovascular diseases: molecular mechanisms and therapeutic prospects. Immunol Rev. 2025;329:e13382. https://doi.org/10.1111/imr.13382.
6. Ma XM, Geng K, Law BY-K, Wang P, Pu YL, Chen Q, Xu HW, Tan XZ, Jiang ZZ, Xu Y. Lipotoxicity-induced mtDNA release promotes diabetic cardiomyopathy by activating the cGAS-STING pathway in obesity-related diabetes. Cell Biol Toxicol. 2023;39:277–99. https://doi.org/10.1007/s10565-021-09692-z.

7. Xiong R, Li N, Chen L, Wang W, Wang B, Jiang W, Geng Q. STING protects against cardiac dysfunction and remodelling by blocking autophagy. Cell Commun Signal. 2021;19:109. https://doi.org/10.1186/s12964-021-00793-0.
8. Zhang Y, Chen W, Wang Y. STING is an essential regulator of heart inflammation and fibrosis in mice with pathological cardiac hypertrophy via endoplasmic reticulum (ER) stress. Biomed Pharmacother. 2020;125:110022. https://doi.org/10.1016/j.biopha.2020.110022.
9. Lu H, Du W, Ren L, Hamblin MH, Becker RC, Chen YE, Fan Y. Vascular smooth muscle cells in aortic aneurysm: from Genetics to mechanisms. J Am Heart Assoc. 2021;10:e023601. https://doi.org/10.1161/JAHA.121.023601.
10. Luo W, Wang Y, Zhang L, Ren P, Zhang C, Li Y, Azares AR, Zhang M, Guo J, Ghaghada KB, Starosolski ZA, Rajapakshe K, Coarfa C, Li Y, Chen R, Fujiwara K, Abe J-I, Coselli JS, Milewicz DM, LeMaire SA, Shen YH. Critical role of cytosolic DNA and its sensing adaptor STING in aortic degeneration, dissection, and rupture. Circulation. 2020;141:42–66. https://doi.org/10.1161/CIRCULATIONAHA.119.041460.
11. Golledge J. Abdominal aortic aneurysm: update on pathogenesis and medical treatments. Nat Rev Cardiol. 2019;16:225–42. https://doi.org/10.1038/s41569-018-0114-9.
12. Martinet W, Knaapen MWM, De Meyer GRY, Herman AG, Kockx MM. Elevated levels of oxidative DNA damage and DNA repair enzymes in human atherosclerotic plaques. Circulation. 2002;106:927–32. https://doi.org/10.1161/01.cir.0000026393.47805.21.
13. Popov SV, Mukhomedzyanov AV, Voronkov NS, Derkachev IA, Boshchenko AA, Fu F, Sufianova GZ, Khlestkina MS, Maslov LN. Regulation of autophagy of the heart in ischemia and reperfusion. Apoptosis. 2023;28:55–80. https://doi.org/10.1007/s10495-022-01786-1.
14. Andreeva L, Hiller B, Kostrewa D, Lässig C, de Oliveira Mann CC, Jan Drexler D, Maiser A, Gaidt M, Leonhardt H, Hornung V. Hopfner, cGAS senses long and HMGB/TFAM-bound U-turn DNA by forming protein-DNA ladders. Nature. 2017;549:394–8. https://doi.org/10.1038/nature23890.
15. Shang G, Zhang C, Chen ZJ, Bai X-C, Zhang X. Cryo-EM structures of STING reveal its mechanism of activation by cyclic GMP-AMP. Nature. 2019;567:389–93. https://doi.org/10.1038/s41586-019-0998-5.
16. Liu S, Cai X, Wu J, Cong Q, Chen X, Li T, Du F, Ren J, Wu Y-T, Grishin NV, Chen ZJ. Phosphorylation of innate immune adaptor proteins MAVS, STING, and TRIF induces IRF3 activation. Science. 2015;347:aaa2630. https://doi.org/10.1126/science.aaa2630.
17. Ding H, Zhang Q, Yang R, Fu L, Jiang H, Zhu Q, Tai S. Aberrant STING activation promotes macrophage senescence by suppressing autophagy in vascular aging from diabetes. iScience. 2024;28:111594. https://doi.org/10.1016/j.isci.2024.111594.
18. Bielak-Zmijewska A, Mosieniak G, Sikora E. Is DNA damage indispensable for stress-induced senescence? Mech Ageing Dev. 2018;170:13–21. https://doi.org/10.1016/j.mad.2017.08.004.
19. Mikuła-Pietrasik J, Niklas A, Uruski P, Tykarski A, Książek K. Mechanisms and significance of therapy-induced and spontaneous senescence of cancer cells. Cell Mol Life Sci. 2020;77:213–29. https://doi.org/10.1007/s00018-019-03261-8.
20. Glück S, Guey B, Gulen MF, Wolter K, Kang T-W, Schmacke NA, Bridgeman A, Rehwinkel J, Zender L, Ablasser A. Innate immune sensing of cytosolic chromatin fragments through cGAS promotes senescence. Nat Cell Biol. 2017;19:1061–70. https://doi.org/10.1038/ncb3586.
21. Yang H, Wang H, Ren J, Chen Q, Chen ZJ. cGAS is essential for cellular senescence. Proc Natl Acad Sci U S A. 2017;114:E4612–20. https://doi.org/10.1073/pnas.1705499114.
22. Li C, Zhang Y, Liu J, Kang R, Klionsky DJ, Tang D. Mitochondrial DNA stress triggers autophagy-dependent ferroptotic death. Autophagy. 2021;17:948–60. https://doi.org/10.1080/15548627.2020.1739447.
23. Paludan SR, Reinert LS, Hornung V. DNA-stimulated cell death: implications for host defence, inflammatory diseases and cancer. Nat Rev Immunol. 2019;19:141–53. https://doi.org/10.1038/s41577-018-0117-0.
24. Pham PT, Fukuda D, Nishimoto S, Kim-Kaneyama J-R, Lei X-F, Takahashi Y, Sato T, Tanaka K, Suto K, Kawabata Y, Yamaguchi K, Yagi S, Kusunose K, Yamada H, Soeki T, Wakatsuki T, Shimada K, Kanematsu Y, Takagi Y, Shimabukuro M, Setou M, Barber GN, Sata M. STING, a cytosolic DNA sensor, plays a critical role in atherogenesis: a link between innate immunity and chronic inflammation caused by lifestyle-related diseases. Eur Heart J. 2021;42:4336–48. https://doi.org/10.1093/eurheartj/ehab249.
25. Lu G-F, Chen S-C, Xia Y-P, Ye Z-M, Cao F, Hu B. Synergistic inflammatory signaling by cGAS may be involved in the development of atherosclerosis. Aging. 2021;13:5650–73. https://doi.org/10.18632/aging.202491.
26. Bi X, Du C, Wang X, Wang X-Y, Han W, Wang Y, Qiao Y, Zhu Y, Ran L, Liu Y, Xiong J, Huang Y, Liu M, Liu C, Zeng C, Wang J, Yang K, Zhao J. Mitochondrial damage-Induced Innate Immune activation in vascular smooth muscle cells promotes chronic kidney Disease-Associated Plaque vulnerability. Adv Sci (Weinh). 2021;8:2002738. https://doi.org/10.1002/advs.202002738.
27. Huang LS, Hong Z, Wu W, Xiong S, Zhong M, Gao X, Rehman J, Malik AB. mtDNA activates cGAS Signaling and suppresses the YAP-Mediated endothelial cell Proliferation Program to Promote Inflammatory Injury. Immunity. 2020;52:475–e4865. https://doi.org/10.1016/j.immuni.2020.02.002.
28. Evrard SM, Lecce L, Michelis KC, Nomura-Kitabayashi A, Pandey G, Purushothaman K-R, d'Escamard V, Li JR, Hadri L, Fujitani K, Moreno PR, Benard L, Rimmele P, Cohain A, Mecham B, Randolph GJ, Nabel EG, Hajjar R, Fuster V, Boehm M, Kovacic JC. Endothelial to mesenchymal transition is common in atherosclerotic lesions and is associated with plaque instability. Nat Commun. 2016;7:11853. https://doi.org/10.1038/ncomms11853.
29. King KR, Aguirre AD, Ye Y-X, Sun Y, Roh JD, Ng RP, Kohler RH, Arlauckas SP, Iwamoto Y, Savol A, Sadreyev RI, Kelly M, Fitzgibbons TP, Fitzgerald KA, Mitchison T, Libby P, Nahrendorf M, Weissleder R. IRF3 and type I interferons fuel a fatal response to myocardial infarction. Nat Med. 2017;23:1481–7. https://doi.org/10.1038/nm.4428.
30. Cao D, Schiattarella GG, Villalobos E, Jiang N, May HI, Li T, Chen ZJ, Gillette TG, Hill JA. Cytosolic DNA sensing promotes Macrophage Transformation and governs myocardial ischemic Injury. Circulation. 2018;137:2613–34. https://doi.org/10.1161/CIRCULATIONAHA.117.031046.
31. Zhang W, Zhang Y, Han L, Bo T, Qi Z, Zhong H, Xu H, Hu L, Chen S, Zhang S. Double-stranded DNA enhances platelet activation, thrombosis, and myocardial injury via cyclic GMP-AMP synthase. Cardiovasc Res. 2024;cvae218. https://doi.org/10.1093/cvr/cvae218.
32. Bouhidel JO, Wang P, Siu KL, Li H, Youn JY, Cai H. Netrin-1 improves post-injury cardiac function in vivo via DCC/NO-dependent preservation of mitochondrial integrity, while attenuating autophagy. Biochim et Biophys Acta (BBA) - Mol Basis Disease. 2015;1852:277–89. https://doi.org/10.1016/j.bbadis.2014.06.005.
33. Han X, Jiang Z, Hou Y, Zhou X, Hu B. Myocardial ischemia-reperfusion injury upregulates nucleostemin expression via HIF-1α and c-Jun pathways and alleviates apoptosis by promoting autophagy. Cell Death Discov. 2024;10:461. https://doi.org/10.1038/s41420-024-02221-x.
34. Ji Z, Guo J, Zhang R, Zuo W, Xu Y, Qu Y, Tao Z, Li X, Li Y, Yao Y, Ma G. ADAM8 deficiency in macrophages promotes cardiac repair after myocardial infarction via ANXA2-mTOR-autophagy pathway. J Adv Res. 2024. https://doi.org/10.1016/j.jare.2024.07.037.
35. Gui X, Yang H, Li T, Tan X, Shi P, Li M, Du F, Chen ZJ. Autophagy induction via STING trafficking is a primordial function of the cGAS pathway. Nature. 2019;567:262–6. https://doi.org/10.1038/s41586-019-1006-9.
36. Gómez-Virgilio L, Silva-Lucero M-D-C, Flores-Morelos D-S, Gallardo-Nieto J, Lopez-Toledo G, Abarca-Fernandez A-M, Zacapala-Gómez A-E, Luna-Muñoz J, Montiel-Sosa F, Soto-Rojas LO, Pacheco-Herrero M. Cardenas-Aguayo, Autophagy: a Key Regulator of Homeostasis and Disease: an overview of Molecular mechanisms and modulators. Cells. 2022;11:2262. https://doi.org/10.3390/cells11152262.

Publisher's note